Journal of Magnetic Resonance 202 (2010) 173–179

Contents lists available at ScienceDirect

Journal of Magnetic Resonance

journal homepage: www.elsevier.com/locate/jmr

A strategy for acquisition and analysis of complex natural abundance ^{33}S solid-state NMR spectra of a disordered tetrathio transition-metal anion

Hans J. Jakobsen [a,*], Henrik Bildsøe [a], Jørgen Skibsted [a], Michael Brorson [b], Peter Gor'kov [c], Zhehong Gan [c]

[a] Instrument Centre for Solid-State NMR Spectroscopy, Interdisciplinary Nanoscience Center (iNANO), Department of Chemistry, Aarhus University, DK-8000 Aarhus C, Denmark
[b] Haldor Topsøe A/S, Nymøllevej 55, DK-2800 Lyngby, Denmark
[c] National High Magnetic Field Laboratory, 1860 East Paul Dirac Drive, Tallahassee, FL 32310, USA

ARTICLE INFO

Article history:
Received 28 August 2009
Revised 30 October 2009
Available online 10 November 2009

Keywords:
^{33}S MAS NMR
WURST polarization transfer
Tetraethylammonium tetrathioperrhenate
QCPMG
Spectral analysis
Quadrupole coupling
Chemical shift anisotropy

ABSTRACT

A strategy, involving (i) sensitivity enhancement for the central transition (CT) by population transfer (PT) employing WURST inversion pulses to the satellite transitions (STs) in natural abundance ^{33}S MAS NMR for two different MAS frequencies (ν_r = 5.0 and 10.0 kHz) at 14.1 T and (ii) a ^{33}S static QCPMG experiment at 19.6 T, has allowed acquisition and analysis of very complex solid-state ^{33}S CT NMR spectra for the disordered tetrathioperrhenate anion ReS_4^- in $[(C_2H_5)_4N][ReS_4]$. This strategy of different NMR experiments combined with spectral analysis/simulations has allowed determination of precise values for two sets of quadrupole coupling parameters (C_Q and η_Q) assigned to the two different S sites for the four sulfur atoms in the ReS_4^- anion in the ratio S1:S2 = 1:3. These sets of C_Q, η_Q values for the S1 and S2 site are quite similar and the magnitudes of the quadrupole coupling constants (C_Q = 2.2–2.5 MHz) are a factor of about three larger than observed for other tetrathiometalates A_2MS_4 (A = NH_4, Cs, Rb and M = W, Mo). In addition, the spectral analysis also leads to a determination of the chemical shift anisotropy (CSA) parameters (δ_σ and η_σ) for the S1 and S2 site, however, with much lower precisions (about 20% error margins) compared to those for C_Q, η_Q, because the magnitudes of the two CSAs (i.e., δ_σ = 60–90 ppm) are about a factor of six smaller than observed for the other tetrathiometalates mentioned above. This large difference in the magnitudes of the anisotropic parameters C_Q and δ_σ for the ReS_4^- anion, compared to those for the WS_4^{2-} and MoS_4^{2-} anions determined previously under identical experimental conditions, accounts for the increased complexity of the PT-enhanced ^{33}S MAS spectra observed for the ReS_4^- anion in this study. This difference in C_Q also contributes significantly to the intensity distortions observed in the outer wings of the CTs when employing PT from the STs under conditions of slow-speed MAS.

1. Introduction

Since sulfur is among the most important non-carbon elements (following nitrogen and oxygen) in a large number of inorganic-, organic-, and bio-materials, it is unfortunate that natural abundance solid-state ^{33}S NMR is considered very challenging within NMR spectroscopy because of the low natural abundance (0.76%), low γ for the ^{33}S (spin $I = 3/2$) quadrupolar nucleus, and its fairly large quadrupole moment (-6.78×10^2 barn). In a recent series of natural abundance ^{33}S MAS NMR studies on ammonium/alkylammonium tetrathiotungstates and molybdates, we presented the first simultaneous determinations of both the quadrupolar coupling parameters (C_Q and η_Q) and anisotropic chemical shift parameters (δ_σ, η_σ, and δ_{iso}), as well as the relative orientation of the ^{33}S tensors for these two anisotropic interactions via solid-state ^{33}S MAS NMR [1–3]. Most importantly, we also showed that employing WURST inversion pulses [4] to the satellite transitions (STs) of the ^{33}S nucleus create a population transfer (PT) from the two $\pm3/2 \leftrightarrow \pm1/2$ STs to the central transition (CT) $+1/2 \leftrightarrow -1/2$ which results in an increase in S/N ratio for the CT by a factor $\geqslant 2$, i.e., a time saving by a factor $\geqslant 4$ for these materials [2]. These advancements in ^{33}S MAS NMR recently allowed us to successfully acquire and fully analyze the most complex natural abundance ^{33}S MAS NMR spectrum observed so far [3]. It is important to note that these natural abundance ^{33}S MAS NMR studies performed at 14.1 T [1–3], all used a probe for 7.5 mm rotors (450 μl sample volume) with a maximum spinning frequency of 6–7 kHz in order to achieve optimum sensitivity at this magnet field strength. Most recently, natural abundance ^{33}S solid-state NMR spectra of some layered transition metal disulfides (in particular for the very important MoS_2, e.g., used in heterogeneous catalysis) have been obtained from static QCPMG [5] experiments at the high magnetic field of 21.1 T [6].

Whereas there has been a tremendous focus on the chemistry, properties, and structural studies of the tetrathiotungstates and

* Corresponding author. Fax: +45 8619 6199.
E-mail address: hja@chem.au.dk (H.J. Jakobsen).

1090-7807/$ - see front matter © 2009 Elsevier Inc. All rights reserved.
doi:10.1016/j.jmr.2009.11.001

-molybdates, much less attention has been paid to the thioanions of other transition metals. In this work we present the results of a natural abundance ^{33}S solid-state NMR investigation of the tetrathioperrhenate anion (ReS_4^-) in the compound $[(C_2H_5)_4N][ReS_4]$, whose structure has been characterized by X-ray diffraction [7]. The present investigation is of interest not only because the transition metal in the ReS_4^- anion is different from tungstate and molybdenum, but also because the crystal structure of $[(C_2H_5)_4N][ReS_4]$ is identified as hexagonal in space group *P6mm* with a 1:1 disorder of both anion and cation [7]. Thus, the structure of the ReS_4^- ion is disordered by two ReS_4^- tetrahedra being superimposed on the C_6 axis sharing the S1 atom and the central Re atom [7], i.e., there is rotational disorder about the unique Re–S1 bond, such that the unique axis is a C_6 axis rather than the expected C_3 axis. In contrast, the tetrathiotungstate and -molybdenum compounds studied so far by ^{33}S MAS NMR [1–3] are all associated with the orthorhombic space group *Pmma* where the MS_4^{2-} (M = W and Mo) anion each exhibits three crystallographically independent S sites, i.e., two of the four S atoms in the MS_4^{2-} ion are equivalent.

Because of the highly complex and quite unexpected appearance observed for the first WURST PT ^{33}S MAS NMR spectrum acquired for the ReS_4^- anion in $[(C_2H_5)_4N][ReS_4]$, a strategy involving ^{33}S MAS for different spinning frequencies at 14.1 T and static QCPMG ^{33}S NMR at 19.6 T combined with spectral simulations has been put forward in order to extract the ^{33}S anisotropic NMR parameters characterizing these spectra. Since this strategy involves a spinning frequency of 10 kHz (or higher), a 4 mm thin-wall zirconia rotor, with the largest possible sample volume (82 μl for sensitivity reasons) and a maximum allowed spinning frequency of just 10 kHz, has been used for some of the experiments. The results obtained by following the steps in this strategy are described here.

2. Experimental

2.1. Material

Tetraethylammonium tetrathioperrhenate, $[(C_2H_5)_4N][ReS_4]$, was synthesized according to the procedure by Goodman and Rauchfuss [8] and isolated as violet crystals. Identity was confirmed by IR [8] and powder X-ray diffraction [7].

2.2. NMR spectroscopy

The WURST PT ^{33}S MAS NMR experiments were performed at 46.06 MHz on a Varian Direct Drive VNMRS-600 spectrometer equipped with an Oxford Instruments 14.1 T wide-bore magnet. The experiments employed Varian/Chemagnetics double- and triple-resonance T3® MAS probes for 7.5 mm o.d. (450 μl sample volume) and 4.0 mm o.d. (82 μl sample volume) rotors, respectively. The magic angle of $\theta = 54.736°$ was adjusted to the highest possible precision (<±0.005°) by ^{14}N MAS NMR at the nearby frequency of 43.34 MHz, using a sample of $NH_4H_2PO_4$ as recently described [9]. The sample of $[(C_2H_5)_4N][ReS_4]$ was spun at MAS frequencies of $\nu_r = 5000$ Hz (7.5 mm rotor) and $\nu_r = 10{,}000$ Hz (4.0 mm rotor) with an ultrahigh precision in ν_r (e.g., <0.5 Hz for the 7.5 mm rotor) employing the experimental setup combined with a Varian/Chemagnetics MAS speed controller as recently described [10]. For both probes the rf field strengths were calibrated for different transmitter power levels using a sample of neat CS_2. Usually an rf field strength of about 13 kHz (i.e., a pulse width of 19.5 μs for a liquid 90° flip angle) was used for both the population transfer (PT) inversion pulses (with a pulse length $T_p = 4$ ms) and excitation of the PT-enhanced magnetization for the CT. For the excitation of the CT magnetization, a pulse width of 5.0 μs (i.e., corresponding to a flip angle of 23°) was employed. Since it has been demonstrated elsewhere [9] that ^{1}H decoupling of residual ^{33}S–^{1}H dipolar couplings in ^{1}H-containing samples is required only for spinning frequencies $\nu_r < 2000$ Hz, ^{1}H decoupling was not employed for the sample in the present experiments. The ^{33}S chemical shifts are referenced to the ^{33}S resonance for neat CS_2, the standard ^{33}S chemical shift reference. In the first WURST PT experiment the offset values for the two inversion pulses applied to the two ^{33}S (±3/2 ↔ ±1/2) satellite transitions (STs) [2] used the same two optimized offsets (about 90 and −85 kHz) as were used [2,3] and as also determined [1] from our earlier studies of the tetrathiotungstates and -molybdates. The reason is that the two WURST PT inversion pulses should preferably be positioned in the region of the two "horns" for the STs as has recently been shown by Wasylishen and coworkers using hyperbolic secant (HS) pulses for PT enhancements of the CTs for quadrupolar nuclei of high NMR sensitivity and with well-known quadrupolar coupling parameters [11]. An evaluation and preliminary analysis of the first acquired WURST PT-enhanced ^{33}S MAS NMR spectrum (*vide infra*) indicated that the ^{33}S quadrupole coupling constants (C_Q) for our ReS_4^- sample are much larger than expected based on our results for the tetrathiotungstates and -molybdates [1–3], and that the offsets for the two inversion pulses should be increased by a factor of about six. Thus, because of the uncertainty in the values for C_Q and η_Q, asymmetrically displaced offsets (580 and −480 kHz, *vide infra*) were used for all WURST PT experiments following the first experiment described above. Otherwise, all other experimental parameters, e.g., the pulse length T_p and bandwidth *bw* for the inversion pulses, and the performance of the actual experiments are identical to and follow the description given elsewhere [2,3].

The static solid-state QCPMG ^{33}S NMR experiments were performed at 63.98 MHz on a Bruker 830-DRX spectrometer equipped with a 19.6 T Magnex narrow-bore (31 mm i.d.) magnet at the NHMFL, Tallahassee, Florida, and employed a homebuilt (NHMFL) broadband 7 mm single-resonance MAS probe (29 mm o.d.) for the use of 7 mm Bruker rotors positioned at the magic angle of 54.74°. Because of a very short $T_2(^{33}S)$ transverse relaxation time it was only possible to observe three spin–echoes for the train of pulses in the QCPMG sequence. Fourier transformation (FT) of the first echo only produces the standard static quadrupolar-echo NMR spectrum (Fig. 3b), which is the spectrum utilized in the analysis of the high-field data in Fig. 3. On the other hand, FT of the full FID of three echoes yields the so-called "spikelet" spectrum [5] in Fig. 3a, which because of the very short $T_2(^{33}S)$ yields no advantage at all with respect to neither S/N nor spectral analysis compared to the standard static quadrupolar-echo spectrum in Fig. 3b. For that reason the "spikelet" spectrum is shown only for comparison with the spectrum of higher quality in Fig. 3b. The QCPMG experiment was performed slightly differently from that outlined in [5] by acquiring full echoes rather than starting from the top of the first echo, which throws half of the signal away. Thus, full-echo acquisition enhances the spin–echo signal by a factor $\sqrt{2}$, but requires application of a large amount of first-order phase correction for phasing of the spectrum.

2.3. Spectral analysis

The PT-enhanced ^{33}S MAS NMR spectra as well as the static QCPMG spectra of the CTs have been analyzed using the STARS simulation software package. STARS (SpecTrum Analysis for Rotating Solids) was developed in our laboratory several years ago [12,13] and the original version of STARS was early on incorporated into Varian's VNMR software for SUN Microsystem computers and has been available from Varian Inc as part of their VNMR Solids software package [14]. The present version of STARS used here has been upgraded during the past few years and is capable of

simultaneously handling spectral parameters (i.e., quadrupole coupling (C_Q and η_Q), chemical shift (δ_{iso}, δ_σ, and η_σ), and Euler angles (ψ, χ, and ξ) relating the relative orientation for these two interactions) for up to nine different nuclear sites in the optimization of a fit to an experimental spectrum. In addition to these spectral parameters, the program can also include (i) deviation from the magic angle, (ii) rf bandwidth, (iii) rf offset, (iv) jitter in spinning frequency [10], and (v) the linewidths (Lorentzian and/or Gaussian) in the iterative fitting procedure. This upgraded version of STARS has been incorporated into both the Varian VnmrJ software running on SUN Microsystems Ultra-5 workstations and the VnmrJ software running on a Linux RedHat PC.

The quadrupole coupling and CSA parameters are defined by

$$C_Q = eQV_{zz}/h \quad \eta_Q = (V_{yy} - V_{xx})/V_{zz} \tag{1}$$

$$\delta_\sigma = \delta_{iso} - \delta_{zz} \quad \eta_\sigma = (\delta_{xx} - \delta_{yy})/\delta_\sigma \tag{2}$$

$$\delta_{iso} = (1/3)(\delta_{xx} + \delta_{yy} + \delta_{zz}) = (1/3)\mathrm{Tr}(\delta) \tag{3}$$

using the convention

$$|\lambda_{zz} - (1/3)\mathrm{Tr}(\lambda)| \geq |\lambda_{xx} - (1/3)\mathrm{Tr}(\lambda)| \geq |\lambda_{yy} - (1/3)\mathrm{Tr}(\lambda)| \tag{4}$$

for the principal elements ($\lambda_{\alpha\alpha} = V_{\alpha\alpha}$, $\delta_{\alpha\alpha}$) of the two tensors. The relative orientation of the two tensors is described by the three Euler angles (ψ, χ, and ξ) which correspond to positive rotations of the CSA principal axis system around $z(\psi)$, the new $y(\chi)$, and the final $z(\xi)$ axis.

3. Results and discussion

3.1. WURST PT-enhanced ^{33}S MAS NMR spectra at 14.1 T

In this section, we describe the strategy, initiated following acquisition of the first WURST PT ^{33}S MAS NMR spectrum for the ReS_4^{2-} anion in $[(C_2H_5)_4N][ReS_4]$ using the 7.5 mm MAS probe. This first experiment employed identical experimental setup parameters (in particular for the two rf offsets, i.e., 90 and −85 kHz) as in our previous investigations on ^{33}S MAS NMR of other tetrathiometalates [2,3] for ν_r = 5.5–6.0 kHz. The observed spectrum (Fig. 1a), expected for the two CTs in the ReS_4^{2-} anion, exhibits an appearance very different from the ^{33}S MAS NMR spectra of the CTs for the MS_4^{2-} anions in our previously studied tetrathiotungstates and -molybdates [1–3]. Furthermore, the experimental spectrum in Fig. 1a shows no immediate resemblance to a spectrum expected for and composed of two overlapping CTs for a spin I = 3/2 quadrupolar nucleus.

Thus, to come up with a possible interpretation of the experimental spectrum in Fig. 1a, numerous trial-and-error simulations have been performed for visual comparison with the experimental spectrum. These simulations all assume two crystallographically different sites (denoted S1 and S2) for the four S atoms in the ReS_4^{2-} anion and with an intensity ratio S1:S2 equal to 1:3, in accordance with the crystal structure for $[(C_2H_5)_4N][ReS_4]$ [7]. In addition, these simulations include qualified trial-and-error variations for the quadrupole coupling and chemical shift anisotropy parameters. For example, the threefold symmetry axis for the S1 site imposes constraints on the values η_Q (=0) and η_σ (=0) in all simulations/iterations for this site. After a decent agreement is reached between a simulated and the experimental spectrum, an optimization of the spectral parameters by iterative fitting simulated spectra to the experimental spectrum is attempted. The optimized simulated spectrum (Fig. 1b) shows a reasonable agreement with the experimental spectrum (Fig. 1a) in the sense that all spectral features are reproduced, however, with some deviations in their relative intensities. The corresponding spectral parameters

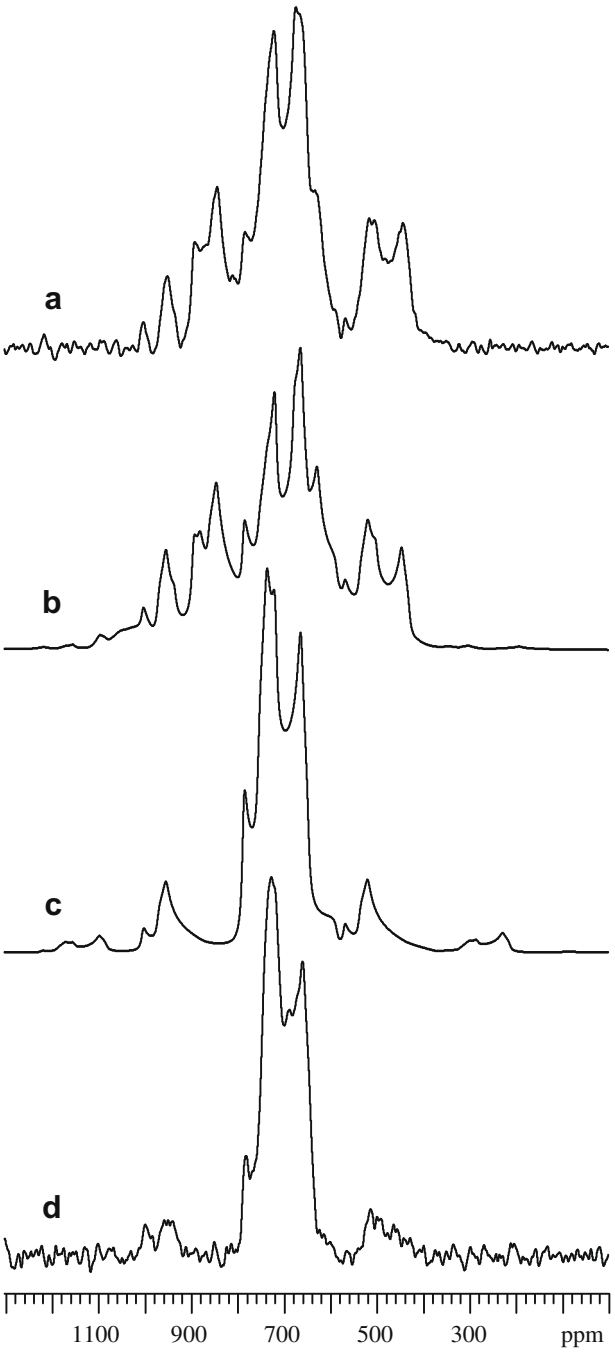

Fig. 1. Natural abundance experimental and simulated ^{33}S MAS NMR spectra (46.06 MHz at 14.1 T) of $[(C_2H_5)_4N][ReS_4]$. (a) Original (first) experimental WURST PT spectrum acquired using a 7.5 mm rotor, ν_r = 5.0 kHz, 466,000 scans, relaxation delay of 0.5 s, offsets for the two WURST inversion pulses of 90 and −85 kHz. (b) Simulation of the experimental MAS NMR spectrum in (a) using the spectral parameters listed in Table 1 (entry I) for a ratio S1:S2 = 1:3, which result from a final iterative optimization of parameters based on trial-and-error simulations (see text). (c) Simulated spectrum for ν_r = 10.0 kHz employing the identical optimized spectral parameters (Table 1 (entry I)) used for the simulation in (b). (d) Experimental WURST PT-enhanced MAS spectrum acquired using a 4 mm rotor, ν_r = 10.0 kHz, 250,000 scans, relaxation delay of 0.5 s, offsets for the WURST pulses of 580 and −480 kHz (see text).

are summarized in Table 1 (entry I) and further simulations show that the error limits for the two C_Q, η_Q parameter sets are quite small (±0.05 MHz and ±0.05, respectively) while they appear large for the two δ_σ values (about ±20 ppm, i.e., about 30% error) and reasonably small for η_σ for the S2 site (about ±0.08). Finally, the

Table 1
^{33}S Quadrupole coupling (C_Q and η_Q) and chemical shift parameters (δ_σ, η_σ, and δ_{iso}) for $[(C_2H_5)_4N][ReS_4]$ determined from natural abundance WURST PT-enhanced ^{33}S MAS and ^{33}S static QCPMG NMR spectra (see text).[a]

Entry experiment	Sites	C_Q (MHz)	η_Q	δ_σ (ppm)	η_σ	δ_{iso} (ppm)	ψ	χ	ξ
I									
14.1 T, MAS	S1	2.21	0.00	68	0.00	808.0	–	0°	–
ν_r = 5.0 kHz	S2	2.51	0.17	80	0.47	773.5	0°	2°	0°
II									
14.1 T, MAS	S1	2.27	0.00	91	0.00	807.5	–	0°	–
ν_r = 10.0 kHz	S2	2.48	0.18	67	0.37	766.4	0°	4°	0°
III									
14.1 T, MAS	S1	2.21	0.00	83	0.00	809.8	–	0°	–
ν_r = 5.0 kHz	S2	2.51	0.17	122	0.51	777.3	0°	4°	0°
IV									
19.6 T, static	S1	2.21	0.00	91	0.00	807.1	–	0°	–
spin–echo	S2	2.51	0.17	67	0.37	766.5	1°	1°	0°

[a] The final best parameter set is shown in entry II. The intensity ratio used in the simulations for the S1 and S2 site is S1:S2 = 1:3, in accordance with the crystal structure for $[(C_2H_5)_4N][ReS_4]$ [7]. Considering the threefold symmetry axis for S1, the crystal structure also imposes constraints on some of the parameters for the S1 site, i.e., η_Q = 0, η_σ = 0, and therefore also the Euler angle χ = 0°, while ψ and ξ become undefined [14] (see text, Section 3.1). Thus, no error limits are given for these S1-site parameters. The error limits for the C_Q values for both the S1 and S2 site are within ±0.05 MHz, as determined along with an error limit of ±0.05 for the S2-site η_Q. These error limits apply for all C_Q, η_Q values in Table 1, entries I–IV. With reference to the text (Sections 3.2–3.4) the error limits for the CSA parameters (δ_σ and η_σ) are much higher compared to the C_Q, η_Q parameters, in particular this holds for the magnitude (δ_σ) of the CSA. For the optimized value for δ_σ (entries II and IV) the error is about 20% while the error limits for the η_σ values is ±0.10. The ψ, χ, ξ Euler angles shown in the table for the S2 site, and which are different from 0°, i.e., the angle χ and ψ (entry IV), are directly obtained from the optimized fitting, while the values of 0° are fixed. The values for the χ angle are clearly somewhat smaller than the determined error limits (i.e., <5°). Thus, our best estimate of the Euler angles for the S2 site will be $\psi = \chi = \xi = 0°$ (see also the text).

iteration also includes an analysis of the relative orientation (i.e., the three Euler angles ψ, χ, and ξ) for the tensors describing the quadrupolar and chemical shift interactions for both the S1 and S2 sites. The constraints for η_Q (=0) and η_σ (=0) for the S1 site imposed by the threefold symmetry axis in the crystal structure [7] imply that the Euler angle $\chi = 0°$ while ψ and ξ are undefined [15]. Thus, the *z* axis of both the quadrupole coupling and CSA tensor for the S1 site coincide with the Re–S1 bond. The results of the combined spectral iterative analysis for the S1 and S2 site show that the optimum value for the S2-site Euler angle χ is close to 0° (<5°), while the ψ and ξ angles are quite insensitive to fairly large deviations from 0°. However, with reference to the optimized values for the ψ and ξ Euler angles obtained from the static spin–echo spectrum at 19.6 T (*vide infra*), we list a value of 0° for these angles in Table 1 for all MAS experiments (entries I–III). The main results of the analysis show that the two $C_Q(^{33}S)$ values for $[(C_2H_5)_4N][ReS_4]$ are approximately a factor of three larger while the two $\delta_\sigma(^{33}S)$ values are about a factor of five smaller than the C_Q and δ_σ values previously determined for the tetrathiometalates A_2MS_4 (A = NH_4, M = W and Mo) [1–3].

Following these preliminary and somewhat uncertain results obtained for ν_r = 5.0 kHz at 14.1 T immediately raised the question: Can the complex ^{33}S MAS NMR spectrum in Fig. 1a be simplified even at 14.1 T by an increase in spinning frequency? Employing the above preliminary spectral parameters in some 14.1 T simulations for spinning frequencies ν_r > 5.0 kHz show that this is indeed the case. In particular, taking the maximum allowed spinning frequency ν_r = 10.0 kHz for the 4 mm thin-wall zirconia rotor (82 μl sample volume) into account, this could for the first time put the 4 mm T3 MAS probe into a critical sensitivity test for natural abundance ^{33}S MAS NMR of the $[(C_2H_5)_4N][ReS_4]$ sample at ν_r = 10.0 kHz and 14.1 T. This follows from the simulated ^{33}S MAS NMR spectrum in Fig. 1c, which shows a highly narrowed simulated spectrum for the two CTs for ν_r = 10.0 kHz at 14.1 T based on the preliminary spectral parameters determined for ν_r = 5.0 kHz (Table 1 (entry I)).

Before acquisition of the corresponding WURST PT-enhanced ^{33}S MAS NMR spectrum for ν_r = 10.0 kHz employing the 4 mm rotor, it was decided to perform a simulation of the full ^{33}S MAS NMR spectrum (i.e., including the satellite transitions) for ν_r = 10.0 kHz, using the same preliminary parameters as for the simulated spectrum in Fig. 1c, in order to evaluate the offset frequencies for the "horns" in the satellite transitions relative to the center part of the spectrum. This simulated spectrum is shown in Fig. 2 and serves to illustrate the actual positions for the two pairs of "horns" for the S1 and S2 sites in the region of their satellite transitions. These positions have recently been demonstrated to be the optimum offset positions for the two inversion pulses [11] with respect to maximum sensitivity gain and minimum lineshape distortion for the CT, and which therefore are to be considered in the acquisition of an experimental PT ^{33}S MAS NMR spectrum of the ReS_4^- anion for ν_r = 10.0 kHz. Fortunately, the optimum offset positions observed for the two S1 and S2 sites (Fig. 2) are quite similar and the offsets chosen for the two WURST inversion pulses are 580 and −480 kHz. These offsets are about a factor of six further away from the CTs compared to the values used to obtain the spectrum in Fig. 1a and originally estimated from ^{33}S MAS NMR spectra of other tetrathiometalates [1–3].

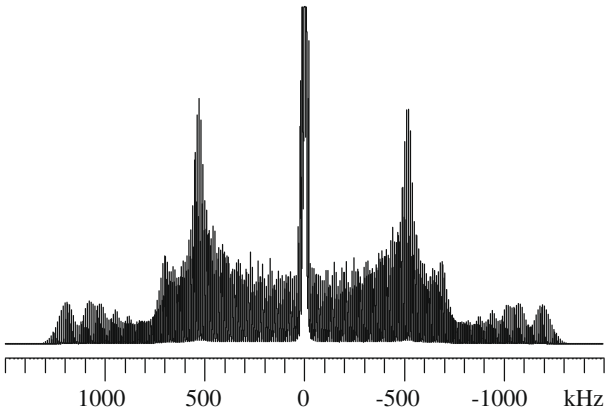

Fig. 2. Simulated ^{33}S MAS NMR spectrum (46.06 MHz at 14.1 T) of $[(C_2H_5)_4N][ReS_4]$ showing the complete MAS spectrum (i.e., the central and satellite transitions) for ν_r = 10.0 kHz and the spectral parameters shown in Table 1 (entry I) and the ratio S1:S2 = 1:3. The central transitions (CTs) have been cut-off at 1/16 of their maximum height. The spectrum serves to illustrate the approximate positions for the "horns" (on the referenced frequency kHz scale) in the satellite transitions, which are important in choosing the optimum offset positions for the WURST inversion pulses (see text).

The actually observed WURST PT-enhanced ^{33}S MAS NMR spectrum acquired for the offsets of 580 and −480 kHz, ν_r = 10.0 kHz at 14.1 T, and employing otherwise identical experimental parameters as used for the spectrum in Fig. 1a, is shown in Fig. 1d. This spectrum exhibits a good resemblance with the predicted simulated spectrum in Fig. 1c based on the preliminary spectral parameters corresponding to the spectra in Fig. 1a and b. In particular, it is noted that the center part of the spectrum (Fig. 1d) very well reproduces the simulated spectrum (Fig. 1c) for the two overlapping CTs (S1:S2 with a relative intensity of 1:3) which confirms the high-quality C_Q, η_Q data estimated for the preliminary spectral parameters. On the contrary, the intensities of the first-order ssbs for the CTs in Fig. 1c and d, which according to our simulations of the ν_r = 10.0 kHz spectrum reflect a strong dependence on the CSA (δ_σ, η_σ, and δ_{iso}) parameters, confirm the very large error limits determined for the CSA parameters obtained from the spectra in Fig. 1a and b. Particularly, the δ_σ value for the high-intensity S2 site appears to be too large based on a comparison of the intensities for the first-order ssbs in Fig. 1c and d. Thus, to take full advantage of the experimental WURST PT ^{33}S MAS (ν_r = 10.0 kHz) spectrum in Fig. 1d, the next step involves an iterative fit (including all relevant spectral parameters) for this spectrum. Now, prior to starting the iterative procedure for the Fig. 1d spectrum, it was decided to seek an independent optimization of the CSA parameters by recording and analyzing a static (non-spinning) spectrum obtained at very high magnetic field in order to include the expected improved CSA data as fixed parameters in the iterative fit of the spectrum in Fig. 1d (ν_r = 10.0 kHz, 14.1 T).

3.2. Static QCPMG ^{33}S NMR spectra at 19.6 T

The experimental QCPMG spectrum produced by FT of only the first spin–echo in the FID corresponds to the standard static spin–echo spectrum and is shown in Fig. 3b. On the other hand FT of the full FID of the three echoes gives the "spikelet" spectrum illustrated in Fig. 3a. In order to extract as precise data as possible for the two sets of CSA parameters, corresponding to the S1 and S2 sites, an iterative fit to the static spin–echo spectrum in Fig. 3b is performed employing the values for C_Q, η_Q, and the three Euler angles (ψ, χ, and ξ) corresponding to the spectra in Fig. 1a and c (Table 1 (entry I)) as fixed parameters. Thus, only the CSA parameters (δ_σ, η_σ, and δ_{iso}) for the S1 and S2 sites are allowed to vary in an optimization for the simulated spectrum. The optimized simulation, shown in Fig. 3c, is in very good agreement with the experimental spectrum (Fig. 3b) and the corresponding spectral parameters are summarized in Table 1 (entry IV). It should be noted that simulated ^{33}S MAS NMR spectra at 19.6 T (63.98 MHz) for ν_r = 8.0 kHz (7.0 mm rotor), using the spectral parameters obtained from the 19.6 T static spectrum (Table 1 (entry IV)), show that variations for δ_σ give no improvements in the error limits for the CSA parameters compared to similar simulations performed for the 14.1 T, ν_r = 10.0 kHz MAS spectra in Fig. 4 and/or the 19.6 T static spectra in Fig. 3.

3.3. Final optimization of ^{33}S parameters from 14.1 and 19.6 T NMR spectra

The optimized δ_σ, η_σ values, determined from the 19.6 T static spin–echo spectrum (Table 1 (entry IV)) are now used as fixed parameters in the iterative fitting of the experimental spectrum in Fig. 1d (ν_r = 10.0 kHz, 14.1 T) through variation of the C_Q, η_Q, δ_{iso}, and Euler angle parameters for the S1 and S2 sites. A comparison of the final optimized simulation with the experimental WURST PT-enhanced ^{33}S MAS NMR spectrum is illustrated in Fig. 4 and the corresponding spectral parameters are summarized in Table 1 (entry II). A slightly improved agreement between the simulated and experimental spectra is observed for the spectra in Fig. 4 compared to the spectra in Fig. 1c and d. It is noted that the values determined for the quadrupolar couplings (C_Q and η_Q) at ν_r = 10.0 kHz are within the error limits (±0.05 MHz) of those obtained from the original ν_r = 5.0 kHz spectrum (Table 1 (entry I)). In contrast, the much larger errors (about 30% error) estimated for the CSA data in the preliminary parameter set is fully confirmed by the quite different CSA data (with an improved error of about 20%) determined from the 19.6 T static spin–echo spectrum. However, it is gratifying to observe a decrease in the magnitude of δ_σ for the S2 site as

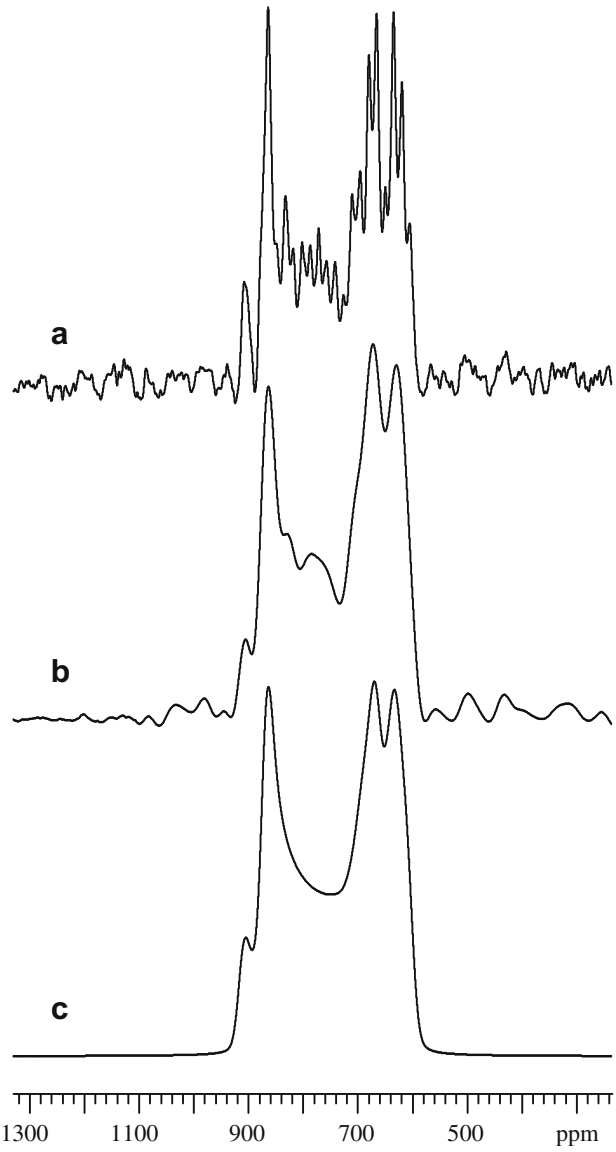

Fig. 3. Static ^{33}S QCPMG NMR spectra of $[(C_2H_5)_4N][ReS_4]$ at 19.6 T (63.98 MHz) obtained as described in Section 2.2. The CT-selective 90° pulse width was 8 μs and the echo train pulses were 16 μs. Five hundred and twelve points (2 μs dwell) were acquired for each full echo with a delay of 62 μs on each side of the refocusing pulses to overcome receiver dead time problems ($\tau_3 = \tau_4$ = 62 μs in the original pulse sequence of Ref. [5]). A relaxation delay of 1.5 s and 131,072 scans were used. Only three echoes are observed because of a very short $T_2(^{33}S)$ relaxation time. (a) "Spikelet" spectrum resulting from FT of the full train of all three echoes and exhibiting a spike separation of 976 Hz in accordance with an evolution time of 1024 μs for the full echo. (b) Standard static spin–echo spectrum obtained by FT of the first echo only. (c) Simulation of the static spin–echo spectrum in (b) using the spectral parameters listed in Table 1 (entry IV), which result from an iterative fit to the spectrum in (b) by variation of the CSA (δ_σ, η_σ, and δ_{iso}) parameters for fixed C_Q, η_Q parameters (Table 1 (entry I)), i.e., used for the spectrum in Fig. 1b and for a ratio S1:S2 = 1:3 (see text).

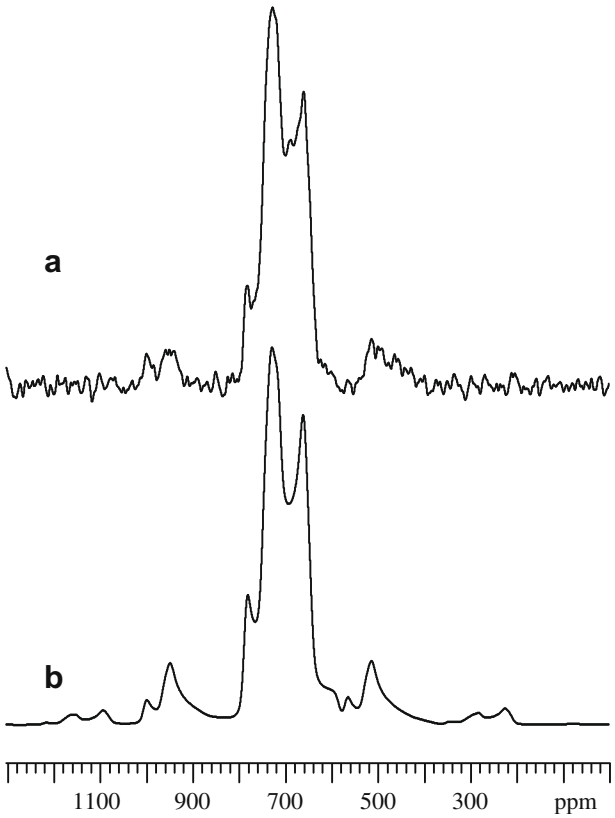

Fig. 4. Experimental and optimized simulated ^{33}S MAS NMR spectra (46.06 MHz at 14.1 T) of $[(C_2H_5)_4N][ReS_4]$ for ν_r = 10.0 kHz. (a) The experimental WURST PT-enhanced MAS spectrum is the same as shown in Fig. 1d. (b) Optimized simulation of the experimental MAS spectrum in (a) using the spectral parameters listed in Table 1 (entry II) which result from an iterative fit to the spectrum in (a) by variation of the quadrupole coupling parameters (C_Q and η_Q) for fixed values of δ_σ and η_σ (Table 1 (entry IV)) as determined from the 19.6 T static spin–echo spectrum and employing a ratio S1:S2 = 1:3 (see text).

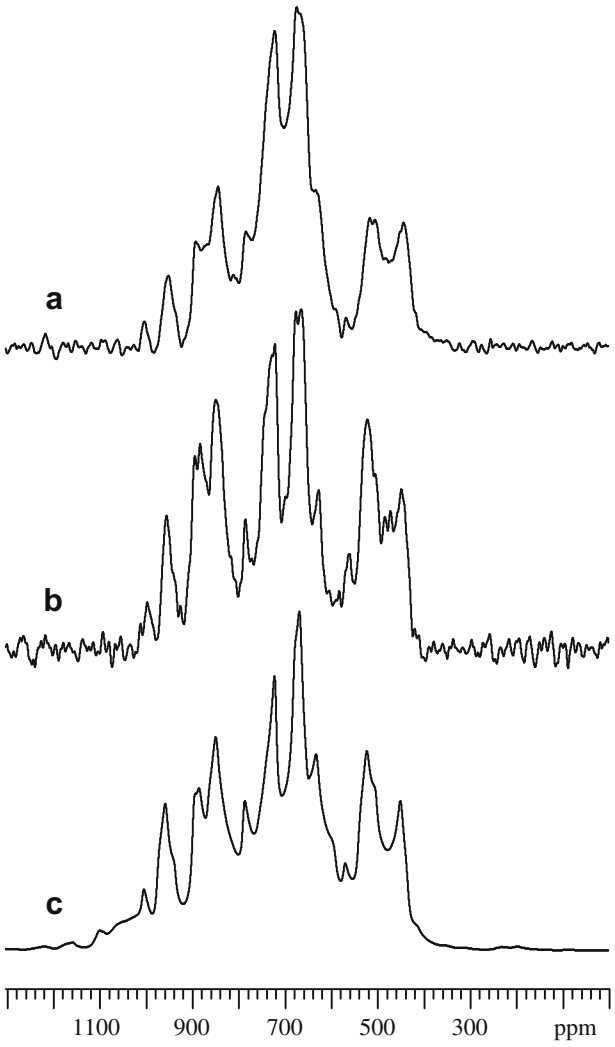

Fig. 5. Natural abundance WURST PT-enhanced ^{33}S MAS NMR spectra (46.06 MHz at 14.1 T) of $[(C_2H_5)_4N][ReS_4]$ obtained for ν_r = 5.0 kHz and different offset positions for the WURST inversion pulses, which serves to illustrate the intensity distortions in the outer wings of the spectra (see text). (a) Same experimental spectrum as shown in Fig. 1a with offsets of 90 and −85 kHz. (b) Experimental spectrum obtained for offsets of 580 and −480 kHz, 163,000 scans, and otherwise identical conditions as for the spectrum in (a). (c) Simulation of the spectrum in (b) using the spectral parameters listed in Table 1 (entry III) which result from an iterative fit to the experimental spectrum in (b) by variation of the CSA parameters for fixed values of the C_Q, η_Q parameters retrieved from the spectrum in Fig. 1a (Table 1 (entry I)) and using a ratio S1:S2 = 1:3.

determined at 19.6 T since this leads to a decrease in the intensity of the first-order ssbs for this site, resulting in an improved agreement between the two spectra in Fig. 4 compared to the two spectra in Fig. 1c and d.

3.4. Intensity distortions for slow MAS

Finally, following the acquisition of the ν_r = 10.0 kHz (4 mm rotor) WURST PT ^{33}S MAS NMR spectrum (Figs. 1d and 4) using the improved offset values of 580 and −480 kHz for the two WURST inversion pulses (*vide supra*), the original 14.1 T PT ^{33}S MAS experiment employing the 7.5 mm rotor for ν_r = 5.0 kHz (Fig. 1a) has been repeated using these improved offsets. This was done in order to hopefully achieve a gain in sensitivity and/or an improvement for the intensities in the outer wings of the spectrum relative to the center part (around 700 ppm), i.e., an intensity distribution, which is related to the magnitude of the CSA. The experimental WURST PT ^{33}S MAS NMR spectrum obtained using the improved offset values for the inversion pulses, and otherwise identical conditions as for the spectrum in Fig. 1a, is shown in Fig. 5b. For comparison the originally observed ν_r = 5.0 kHz spectrum (Fig. 1a) is shown in Fig. 5a. This clearly illustrates an increase in the intensities for the outer wings relative to the center part in the spectrum obtained using the improved, large offsets for the inversion pulses (Fig. 5b). An iterative fit to the experimental spectrum in Fig. 5b, employing the C_Q, η_Q values determined from the spectrum in Fig. 1a (Table 1 (entry I)) as fixed parameters and only allowing optimization for the CSA parameters, is shown in Fig. 5c and the corresponding spectral parameters are listed in Table 1 (entry III). As expected from the increased intensities in the outer wings of the spectrum in Fig. 5b, the optimized δ_σ value determined for the dominating S2 site (δ_σ = 122 ppm) turns out to be almost a factor of two larger than the value (δ_σ = 67 ppm) determined from the 19.6 T static spectrum, a value which also gives an excellent fit for the ν_r = 10.0 kHz spectrum in Fig. 4. Further simulations of both the 19.6 T static (Fig. 3) and 14.1 T ν_r = 10.0 kHz (Fig. 4) spectra, employing δ_σ = 122 ppm for the S2 site, show that this value is definitely too large to produce acceptable fits.

The above observations show that highly distorted central transitions (CTs), resulting from the use of too slow spinning frequencies (ν_r) for narrowing relatively strong second-order broadened CTs, not only complicates the interpretation/analysis of the spectrum, but also leads to intensity distortions within the spectral pattern observed using PT methods such as WURST inversion pulses.

Moreover, these PT intensity distortions are highly influenced by the offset positions used for the inversion pulses. It is noted that observation of intensity distortions are also possible for second-order quadrupolar broadened CTs, observed by PT methods and employing sufficiently high MAS frequencies which exceed the full width of the CT, in case the experimental conditions are not properly optimized [11].

4. Conclusions

WURST PT-enhanced ^{33}S MAS NMR for two spinning frequencies (ν_r = 5.0 and 10.0 kHz) on a mid-field spectrometer (14.1 T) combined with static QCPMG ^{33}S NMR on a high-field spectrometer (19.6 T) has allowed acquisition and analysis of highly complex natural abundance solid-state ^{33}S NMR spectra of the disordered tetrathioperrhenate anion, ReS_4^-, in $[(C_2H_5)_4N][ReS_4]$. The parameters, resulting from the outlined strategy and spectral analysis of the experiments for the ReS_4^- anion, differ substantially from those determined recently for other tetrathio transition-metal anions, as for example the ammonium [1–3] and alkalimetal tetrathiotungstates and -molybdates (MS_4^{2-}, M = W and Mo). Thus, the values of the quadrupolar coupling constants (C_Q) for the S1 and S2 sites in the ReS_4^- anion are both about a factor of three larger than observed for the MS_4^{2-} (M = W and Mo) anions while the magnitudes of the CSA interaction (δ_σ) for the two sites in ReS_4^- are both about a factor of five smaller compared to the values for the MS_4^{2-} anions. These values for the ^{33}S(C_Q, η_Q) and ^{33}S(δ_σ, η_σ, δ_{iso}) parameters (Table 1) are responsible for the high degree of complexity for the ^{33}S MAS NMR spectra observed here for the ReS_4^- anion employing our standard 14.1 T ^{33}S MAS (7.5 mm rotor) NMR equipment and coped with in this study. Furthermore, the increase in C_Q and decrease for δ_σ to quite small values for the ReS_4^- anion also account for the very good error limits obtained for the C_Q, η_Q parameters and rather poor error limits (about 20% error) for the optimum CSA parameters. Finally, it is pointed out that the use of slow MAS speeds, i.e., insufficient to completely narrow the static second-order lineshape for the CT to its MAS lineshape, leads to intensity distortions in the outer wings for the CT lineshapes in the WURST PT experiments and thereby prevents an improved determination for the precision of the CSA parameters.

Acknowledgments

The use of the facilities at the Instrument Centre for Solid-State NMR Spectroscopy, Aarhus University, sponsored by the Danish Natural Science Research Council, the Danish Technical Science Research Council, Teknologistyrelsen, Carlsbergfondet, and Direktør Ib Henriksens Fond, and the use of the high-field NMR facility at the National High Magnetic Field Laboratory supported by National Science Foundation (DMR-0084173) are acknowledged.

References

[1] H.J. Jakobsen, A.R. Hove, H. Bildsøe, J. Skibsted, M. Brorson, Advancements in natural abundance solid-state ^{33}S MAS NMR: characterization of transition-metal M=S bonds in ammonium tetrathiometalates, Chem. Commun. (2007) 1629–1631.
[2] M.R. Hansen, M. Brorson, H. Bildsøe, J. Skibsted, H.J. Jakobsen, Sensitivity enhancement in natural-abundance solid-state ^{33}S MAS NMR spectroscopy employing adiabatic inversion pulses to the satellite transitions, J. Magn. Reson. 190 (2008) 316–326.
[3] H.J. Jakobsen, H. Bildsøe, J. Skibsted, M. Brorson, B.R. Srinivasan, C. Näther, W. Bensch, New opportunities in acquisition and analysis of natural abundance complex solid-state ^{33}S MAS NMR spectra: $(CH_3NH_3)_2WS_4$, Phys. Chem. Chem. Phys. 11 (2009) 6981–6986.
[4] E. Kupce, R. Freeman, Adiabatic pulses for wideband inversion and broadband decoupling, J. Magn. Reson. A 115 (1995) 273–276.
[5] F.H. Larsen, H.J. Jakobsen, P.D. Ellis, N.C. Nielsen, Sensitivity-enhanced quadrupolar-echo NMR of half-integer quadrupolar nuclei. Magnitudes and relative orientation of chemical shielding and quadrupolar coupling tensors, J. Phys. Chem. A 101 (1997) 8597–8606.
[6] A. Sutrisno, V.V. Terskikh, Y. Huang, A natural abundance ^{33}S solid-state NMR study of layered transition metal disulfides at ultrahigh magnetic field, Chem. Commun. (2009) 186–188.
[7] A. Müller, E. Krickemeyer, H. Bögge, M. Penk, D. Rehder, $[ReS_4]^-$, $[ReS_9]^-$, $[ReOS_8]^-$: simple synthesis with S_x^{2-} solutions, structural data, and $^{185/187}$Re-NMR studies, Chimia 40 (1986) 50–52.
[8] J.T. Goodman, T.B. Rauchfuss, Tetraethylammonium tetrathioperrhenate $Et_4N(ReS_4)$, Inorg. Synth. 33 (2002) 107–110.
[9] H.J. Jakobsen, A.R. Hove, H. Bildsøe, J. Skibsted, Satellite transitions in natural abundance solid-state ^{33}S MAS NMR of alums – sign change with zero-crossing of C_Q in a variable temperature study, J. Magn. Reson. 180 (2006) 170–177.
[10] H.J. Jakobsen, A.R. Hove, H. Bildsøe, J. Skibsted, M. Brorson, Long-term stability of rotor-controlled MAS frequencies to 0.1 Hz proved by ^{14}N MAS NMR experiments and simulations, J. Magn. Reson. 185 (2007) 159–163.
[11] R. Siegel, T.T. Nakashima, R.E. Wasylishen, Sensitivity enhancement of NMR spectra of half-integer spin quadrupolar nuclei in solids using hyperbolic secant pulses, J. Magn. Reson. 184 (2007) 85–100, and references cited therein to various versions of the DFS, RAPT, and HS techniques.
[12] H.J. Jakobsen, J. Skibsted, H. Bildsøe, N.C. Nielsen, Magic-angle spinning NMR spectra of satellite transitions for quadrupolar nuclei in solids, J. Magn. Reson. 85 (1989) 173–180.
[13] J. Skibsted, N.C. Nielsen, H. Bildsøe, H.J. Jakobsen, Satellite transitions in MAS NMR of quadrupolar nuclei, J. Magn. Reson. 95 (1991) 88–117.
[14] Varian Manual, STARS (SpecTrum Analysis for Rotating Solids), Publication No. 87-195233-00, Rev. A0296, 1996.
[15] J. Skibsted, N.C. Nielsen, H. Bildsøe, H.J. Jakobsen, ^{51}V MAS NMR Spectroscopy: determination of quadrupole and anisotropic shielding tensors, including the relative orientation of their principal-axis systems, Chem. Phys. Lett. 188 (1992) 405–412.